Journal of Statistical Physics, Vol. 33, No. 1, 1983

Invariant Curves, Attractors, and Phase Diagram of a Piecewise Linear Map with Chaos

Tamás Tél[1]

Received March 29, 1983

We introduce equations describing the invariant curves associated with periodic points in a wide class of two-dimensional invertible maps, which in the special case of the map $T(x, z) = (1 - a|x| + bz, x)$ can be solved by analytical methods. In the dissipative case several branches of the separatrices of the fixed points, as well as, of the period-2 and -4 points, are constructed. The regions of the parameter space where a given type of strange attractor exists are located. We point out that the disappearance of homoclinic intersections between the separatrices of the fixed point and that of heteroclinic intersections between the unstable manifolds of the period-2 points and the stable manifold of the fixed point may occur separately, and the latter leads already to the appearance of a two-piece strange attractor. This phenomenon may happen at weak dissipation in other maps, too. In the conservative case $b = 1$ separatrices and certain invariant tori are calculated.

KEY WORDS: Two-dimensional map; invariant curves; homoclinic and heteroclinic points; evolution of strange attractors; phase diagram; invariant tori.

1. INTRODUCTION AND SUMMARY

The simplest mathematical objects which may exhibit chaotic behavior are one- and two-dimensional maps simulating the recursion of intersection points of trajectories in dynamical systems with a Poincaré surface. Owing

[1] Fachbereich Physik, Universität Essen GHS, Postfach 103764, D-4300 Essen 1, Federal Republic of Germany.
[2] On leave from Institute for Theoretical Physics, Eötvös University, Budapest, Hungary.

0022-4715/83/1000-0195$03.00/0

to the nonlinearity of these maps, however, the investigations are, at least partially, restricted to numerical or perturbative methods.[1,2]

It has been recognized only quite recently that for maps characterized by piecewise linear functions the construction of explicit solutions is possible. One such example is the Kaplan–Yorke map[3] where analytic results have been obtained for some correlation functions[4] and for the invariant measure.[5] The calculations have been extended to a stochastic version of the model[6,7] as well. Another example, we consider in detail in this paper is the two-dimensional invertible map introduced by Lozi.[8] It belongs to a broader family of maps, including the famous Hénon model,[9,10] the members of which are expected, at least in the chaotic region, to exhibit certain topological similarities. It is the piecewise linear map, however, which possesses the simplest strange attractor being the product of pieces of straight lines by a Cantor set.[8] Owing to this simplicity again explicit calculations are possible, and the qualitative picture emerging from this model may have some relevance to other members of the family, too. As for the mathematical properties of the particular map, Misiurewicz[11] has proven the existence of a strange attractor in a given range of parameters (and the topological mixing along it). In two previous papers[12,13] we presented a method for solving the equations for the invariant curves associated with the fixed points and period-2 points and explicitly constructed several branches of the stable and unstable manifolds. A three-dimensional piecewise linear map has been investigated in Ref. 14.

Stable and unstable manifolds (separatrices) play an essential role in dynamical systems as chaotic behavior is related in both dissipative and Hamiltonian cases to the emergence of homoclinic points, i.e., of intersection points between the stable and unstable manifolds of the same hyperbolic point.[1] Strange attractors of dissipative chaotic systems are associated with the unstable manifolds of hyperbolic points. As the unstable manifolds of periodic points are expected to run "parallel" to that of a fixed point, one-piece strange attractors appear to be the closure of the unstable manifold of hyperbolic fixed points.[15–18,2] On the other hand, the existence of heteroclinic points, i.e., intersection points with the stable manifold of another fixed point, destroys the attractor. Thus, one may conclude that if the unstable manifold of a fixed point is bounded and possesses no heteroclinic points, then its closure is a one-piece strange attractor as long as homoclinic points are present. The investigations, however, supporting this rule come from systems with relatively strong dissipation. Through the example of the piecewise linear map we shall show that the above condition is not sufficient. In the case of relatively weak dissipation it may happen that the unstable manifolds of period-2 points

are not crossed by the stable manifold of the fixed point, although the latter still possesses homoclinic points, and then the strange attractor is the closure of the unstable manifolds of the period-2 points (a two-piece object). In other words, by changing a control parameter of the system one generally reaches a point beyond which no heteroclinic intersections exist between the unstable manifolds of the period-2 points and the stable one of the fixed point and, in the case of strong dissipation, homoclinic intersections along the separatrices of the fixed point cease at the same value.[15] We illustrate in the following that the two events may occur separately. This can lead to the peculiar phenomenon that at a fixed dissipation strength a two-piece strange attractor may exist even if a one-piece strange attractor cannot be present.

The explicit construction for the piecewise linear model makes it possible to establish a phase diagram, i.e., to specify in which region of the parameter space the different attractors exist. In the case of extremely strong dissipation (one-dimensional case) the strange attractor possesses a sequence of bifurcations into 2^n bands when lowering the control parameter. Our results indicate that this property does not remain valid, at least in the piecewise linear map, for cases with less strong dissipation.

Furthermore, in the Hamiltonian (or conservative) limit we construct several branches of the separatrices of fixed points, show that they have homoclinic intersections, and for closed invariant curves of period-2 points we prove they are ellipses.

The paper is organized as follows. In Section 2 we introduce equations describing the invariant curves associated with periodic points in a broad class of two-dimensional invertible maps. In the conservative limit some general symmetry relations are found. Then, we turn to the piecewise linear map and after determining some of its periodic points and their stability region (Section 3), we discuss the method for solving the equations of invariant curves in Section 4. The structure of the strange attractor at the standard values of parameters is investigated. We illustrate that the unstable manifolds of the periodic points are indeed parallel to that of one of the fixed points, and that they possess homoclinic intersections. The modification of the strange attractor by varying a control parameter is examined in Section 5. The critical situations where heteroclinic points appear between the invariant curves of the fixed points and when homoclinic points cease to exist along the separatrices of the fixed point, as well as of period-2 and -4 points, is considered. Next, we discuss the structural instability of the unstable manifolds of the period-2 points and show that in the region characterized by a more compact form it may happen that these manifolds have no heteroclinic intersections with that of the fixed point in spite of the

fact that homoclinic points still exist between the separatrices of the fixed point. Section 7 is devoted to the conservative limit.

2. EQUATIONS FOR THE INVARIANT CURVES IN A CLASS OF TWO-DIMENSIONAL MAPS

We consider the class of mappings of the plane into itself defined by the transformation

$$T\begin{pmatrix} x \\ z \end{pmatrix} = \begin{pmatrix} T_x(x,z) = f(x) + bz \\ T_z(x,z) = x \end{pmatrix} \tag{2.1}$$

where f denotes a single-humped symmetric function. The Jacobian of the map is constant, $-b$. The case of $|b| < 1$ corresponds to the dynamics of a dissipative system, and that of $|b| = 1$ to a conservative (Hamiltonian) system. In the limit $b \to 0$ the map becomes one dimensional. The transformation is invertible for $b \neq 0$, and after a change of variables $x \leftrightarrow -z$ it has the same form as (2.1), i.e.,

$$\tilde{T}\begin{pmatrix} x \\ z \end{pmatrix} = \begin{pmatrix} \tilde{T}_x(x,z) = \tilde{f}(x) + \tilde{b}z \\ \tilde{T}_z(x,z) = x \end{pmatrix} \tag{2.2}$$

with

$$\tilde{f}(x) = \frac{1}{b} f(x), \qquad \tilde{b} = \frac{1}{b} \tag{2.3}$$

For

$$f(x) = 1 - ax^2 \tag{2.4}$$

we recover the Hénon model discussed extensively in the literature.[15,18–25] The particular example we shall treat is

$$f(x) = 1 - a|x| \tag{2.5}$$

which corresponds to the piecewise linear map introduced by Lozi.[8] As we shall see, inside the chaotic region the two maps exhibit qualitative similarities in the topological structure of their invariant curves.

The equations for the invariant manifolds follow immediately from (2.1). Let us consider the set of invariant curves of the n-cycle points G_i with sequence $G_1 \to G_2 \to \cdots \to G_n \to G_1$. It is natural to assume that this object is described by n continuous, generally multivalued, functions $f_1^*, \ldots, f_n^*$ such that the curve $x = f_i^*(z)$ belongs to G_i. Applying (2.1) to the points of this manifold, we obtain new points with coordinates $x' = f(x) + bf_i^{*-1}(x)$ and $z' = x$, where f_i^{*-1} denotes the inverse of f_i^*, generally multivalued too. As, however, the image must lie on the invariant curve

around G_{i+1}, $x' = f^*_{i+1}(z')$ holds and we find the set of equations

$$f^*_{i+1}(z) = f(z) + bf^{*-1}_i(z), \qquad i = 1, \ldots, n \tag{2.6}$$

specifying the functions f^*_i. Here the independent variable is denoted again by z, and, of course, $f^*_{n+1} = f^*_1$ is understood. Similar equations follow from the inverted map (2.2). Taking into consideration that the order of sequence of the n cycle is now opposite, one obtains

$$\tilde{f}^*_i(z) = \tilde{f}(z) + b\tilde{f}^{*-1}_{i+1}(z), \qquad i = 1, \ldots, n \tag{2.7}$$

The curve $x = \tilde{f}^*_i(z)$ represents an invariant manifold associated with $\tilde{G}_i$, where $\tilde{G}_i$ denotes the same point in $\tilde{T}$ as does G_i in T.

For dissipative maps Eq. (2.6) with $n = 1$ has been used first by Bridges and Rowlands[26] to obtain an approximate expression for the Hénon attractor. For describing other invariant manifolds of fixed points it has been applied in Refs. 18 and 12. The case of period-2 points has been discussed recently.[13] For Hamiltonian systems, however, Eq. (2.6) with $n = 1$ was used already more than 12 years ago by McMillan[27] to calculate invariant curves around elliptic fixed points (in fact, he considered the limit $b = -1$).

Equations (2.6) and (2.7) have the same content; therefore simplicity and directness govern which of the two is to be solved. We shall discuss a method which is self-generating when applied to the unstable manifolds described by (2.6), but not for the stable ones. The advantage of Eq. (2.7) lies in the fact that in the inverted map the stable manifolds become unstable and thus the same method if performed in representation (2.7) generates the branches of the stable manifolds of the original map.[12] Formally, by knowing any of the solutions $f^*_i(z)$ of (2.6),

$$\tilde{f}^*_i(z) = -f^{*-1}_i(-z) \tag{2.8}$$

will be a solution of (2.7).

This relation leads to important consequences for Hamiltonian systems. We investigate here the limit $b = 1$ only; however, for $b = -1$ see Ref. 27. Let us consider first the case of the invariant manifolds of hyperbolic fixed points. If f^{*u}_+ belongs to the unstable manifold of the fixed point H_+, lying in the first quadrant, the corresponding $\tilde{f}^{*u}_+$ should describe the stable manifold of the other fixed point H_- (in the third quadrant) as the form of the transformations T and $\tilde{T}$ are now the same and $\tilde{H}_+$ is just H_- and vice versa. Thus

$$f^{*s}_-(z) = -f^{*u-1}_+(-z) \tag{2.9}$$

and similarly for the other two separatrices. This means that the stable (unstable) manifold of one of the fixed points and the unstable (stable)

manifold of the other one are of the same form in conservative systems belonging to the class (2.1) with $b = 1$. Applying now (2.8) to a case when the period-2 points F_1, F_2 are elliptic and, as typical, they lie in the second and fourth quadrant, we find

$$f^*_{1(2)}(z) = -f^{*-1}_{1(2)}(-z) \tag{2.10}$$

since $\tilde{F}_{1(2)} = F_{1(2)}$ and T and $\tilde{T}$ coincide. Equation (2.10) expresses a symmetry property of the invariant curves of elliptic period-2 points in systems with $b = 1$.

Let us finally consider the periodic points $G_1, \ldots, G_n$ themselves. As a consequence of the second equation of (2.1) their coordinates should be written in the form $(x_1^{(n)}, x_n^{(n)}), (x_2^{(n)}, x_1^{(n)}), \ldots, (x_n^{(n)}, x_{n-1}^{(n)})$. The set of these points is invariant; therefore, it follows from the argument above that the unknown coordinates are solutions of the set

$$x_{i+1}^{(n)} = f\left(x_i^{(n)}\right) + bx_{i-1}^{(n)}, \qquad i = 1, \ldots, n \tag{2.11}$$

$(x_{n+1}^{(n)} = x_1^{(n)},\ x_0^{(n)} = x_n^{(n)})$. By means of these equations one can specify with relative ease periodic points of higher order.

3. PERIODIC POINTS AND THEIR STABILITY IN THE PIECEWISE LINEAR MAP

We turn now to the particular model defined by (2.5) and focus our attention on the most interesting part of the parameter space specified by $1 < a \leqslant 2$ and $0 \leqslant b \leqslant 1$. First, we discuss periodic points which are relevant in later sections.

In the region defined above two fixed points exist:

$$H_+ : \left(x^*_+ = z^*_+ = \frac{1}{1-b+a}\right), \qquad H_- : \left(x^*_- = z^*_- = \frac{1}{1-b-a}\right) \tag{3.1}$$

From the derivative matrix of the map we find the eigenvalues at H_+ to be

$$\lambda^u_+ = -\left[a + (a^2+4b)^{1/2}\right]/2 \tag{3.2}$$

$$\lambda^s_+ = -\left[a - (a^2+4b)^{1/2}\right]/2 \tag{3.3}$$

$|\lambda^u_+| > 1$ and $|\lambda^s_+| < 1$ for $a > 1 - b$, consequently in the whole region of interest. At H_- we obtain

$$\lambda^u_- = -\lambda^u_+, \qquad \lambda^s_- = -\lambda^s_+ \tag{3.4}$$

as eigenvalues. Thus both fixed points are hyperbolic.

The coordinates of the period-2 points differing from H_+ and H_- follow easily from (2.11) to be

$$x_1^{(2)} = (1-b+a)/N_2, \qquad x_2^{(2)} = (1-b-a)/N_2 \tag{3.5}$$

where

$$N_2 = (1-b)^2 + a^2 \tag{3.6}$$

The corresponding eigenvalues are

$$\lambda_{\pm}^{(2)} = b - a^2/2 \mp a(a^2 - 4b)^{1/2}/2 \tag{3.7}$$

They are less than 1 in modulus if

$$a < a^{(2)} \equiv 1 + b \tag{3.8}$$

i.e., the 2-cycle is stable in this region, otherwise unstable (with hyperbolic points). Entering the domain

$$a < \tilde{a}^{(2)} \equiv 2\sqrt{b} \tag{3.9}$$

the stable nodes become stable spirals.

Among the four-cycles a central role is played by the one for which $x_2^{(4)} < 0$ and the other coordinates are positive. From (2.11) we obtain

$$\begin{aligned} x_1^{(4)} &= \left[(1-b^2)(1+b-a) + a^2(1+b+a)\right]/N_4 \\ x_2^{(4)} &= \left[(1+b)^2 + a^2\right](1-b-a)/N_4 \\ x_3^{(4)} &= \left[(1-b^2)(1+b+a) - a^2(1+b-a)\right]/N_4 \\ x_4^{(4)} &= \left[1-(a+b)^2\right](1+b-a)/N_4 \end{aligned} \tag{3.10}$$

with

$$N_4 = (1-b^2)^2 + a^4 \tag{3.11}$$

As $x_4^{(4)}$ must be nonnegative, this 4-cycle is defined only for $a \geqslant 1 + b$. The eigenvalues are given by

$$\lambda_{\pm}^{(4)} = b^2 - a^4/2 \mp a^2(a^4 - 4b^2)^{1/2}/2 \tag{3.12}$$

$|\lambda_+^{(4)}| > 1$, $|\lambda_-^{(4)}| < 1$ in the region of existence, the cycle is unstable.

The 6-cycle with $x_2^{(6)}, x_4^{(6)} < 0$ (otherwise positive) will be important in our argument. We give the coordinates of that point only which lies above the diagonal in the first quadrant:

$$\begin{aligned} x_1^{(6)} = \{&1 + b - a + a^2b^2(1-b-a) + (a^2+b^2)(1-b+a) \\ &+ \left[2ab(a+b^2) - a^4 - b^4\right](1+b+a)\}/N_6 \end{aligned} \tag{3.13}$$

$$\begin{aligned} x_6^{(6)} = \{&(1+b^2)\left[1-(a+b)^2\right](1+b-a) \\ &+ (a^4 - 4a^2b + b^2)(1-b-a)\}/N_6 \end{aligned} \tag{3.14}$$

with

$$N_6 = (1 - b^3)^2 + a^2(a^2 + b)(3b - a^2) \tag{3.15}$$

This cycle is unstable, too.

4. CONSTRUCTION OF STABLE AND UNSTABLE MANIFOLDS. THE STRUCTURE OF THE STRANGE ATTRACTOR AT STANDARD PARAMETER VALUES

The common idea in calculating the invariant manifolds associated with period-n points of the piecewise linear map is to assume that the curve is a straight line in a finite (not only infinitesimal) neighborhood of the point in question. This assumption works since the map acts linearly in a whole half-plane. First, one specifies straight lines going through the periodic point G_i by writing

$$f_i^* : x = x_i^{(n)} + \lambda_i^{(n)}\left(z - x_{i-1}^{(n)}\right), \qquad i = 1, \ldots, n \tag{4.1}$$

where $x_i^{(n)}$ denote the coordinates given by (2.11). After substituting these forms into (2.6) the slopes can be determined. Assuming the straight lines are defined in the half-plane of the corresponding periodic point, the precise range of validity of the branches follows from (2.6). Moreover, for the unstable manifolds the same equation generates further pieces of straight line segments of the separatrices.

To be more precise, let us start with the unstable manifold W_+^u of the fixed point H_+.[12] We set x_+^* as $x_1^{(1)}$ in Eq. (4.1) (now $n = 1$). It follows then from (2.6) that $\lambda_1^{(1)}$ takes the value λ_+^u of (3.2). The property that the slope of the straight line is just the eigenvalue of the transformation is a consequence of having the eigenvector in the form of $(\lambda_+^u, 1)$ due to the second equation of (2.1). Because the straight line is defined in the region $z \geqslant 0$, f_+^u has a maximum value

$$c_+^* = (1 - \lambda_+^u)x_+^* \tag{4.2}$$

Consequently, the inverse ranges up to $z = c_+^*$ only, which according to (2.6) restricts the region of validity of (4.1). Thus, (4.1) describes a branch of W_+^u between the points $P_0 : (c_+^*, 0)$ and $P_1 : (1 - ac_+^*, c_+^*)$, where P_1 is just the image of P_0. Since $|\lambda_+^u| > 1$, the inverse of this branch is defined along a longer interval as the branch itself. This fact makes it possible to construct a new branch in the region $1 - ac_+^* \leqslant z \leqslant 0$. Following (2.6), we have to add the inverse of (4.1) multiplied by b to $1 + az$, which results in

$$x = c_+^* + (2a + \lambda_+^u)z \tag{4.3}$$

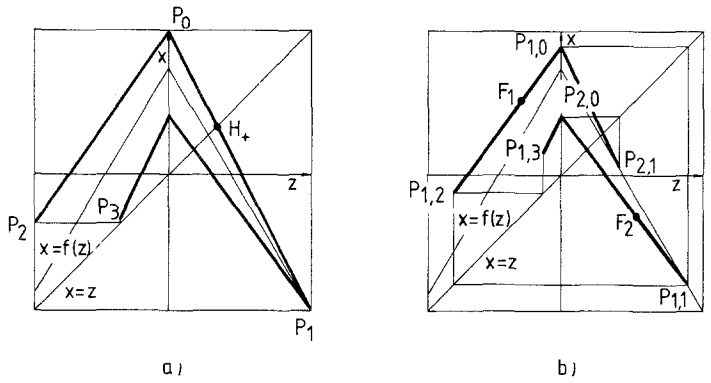

Fig. 1. (a) The first branches of the unstable manifold $W_{\pm}^{u}$; (b) The first branches of the unstable manifolds associated with the period-2 points F_1, F_2.

The range of (4.3) is limited by P_2, the second iterate of P_0, and P_0 itself (Fig. 1a). The inverse of the two-branch object contains a new branch as compared to the previous step, namely, that corresponding to $\overline{P_2P_0}$. This branch then, through (2.6), specifies a new one (Fig. 1a). As, however, the inverse of this object contains again new branches, we have to reiterate the procedure which can be most easily performed by means of a graphical construction.

A similar self-generating procedure works for the unstable manifold W_{-}^{u} of the other fixed point, H_{-}, too. The only modification is that the first branch going through H_{-} is not bounded from the left. All the further branches are already confined into those of W_{+}^{u}.

As for the stable separatrices, it follows from (4.1) that the straight lines with $\lambda_1^{(1)} = \lambda_{\pm}^{s}$ ((3.3), (3.4)) cross the z axis at

$$d_{\pm}^{*} = x_{\pm}^{*}(1 - 1/\lambda_{\pm}^{s}) \tag{4.4}$$

In the inverted map (2.2) the lines have slopes greater than 1 in modulus, thus we find a similar situation in $\tilde{T}$ as in T above. From (2.7) one obtains for the first two branches of $W_{\pm}^{s}$

$$x = \lambda_{\pm}^{s}(z - d_{\pm}^{*}) \tag{4.5}$$

$$x = \frac{z - d_{\pm}^{*}}{1/\lambda_{\pm}^{s} \mp 2a/b} \tag{4.6}$$

The end points of these objects and further parts of the stable manifolds are to be constructed in an analogous way to that used for $W_{\pm}^{u}$.

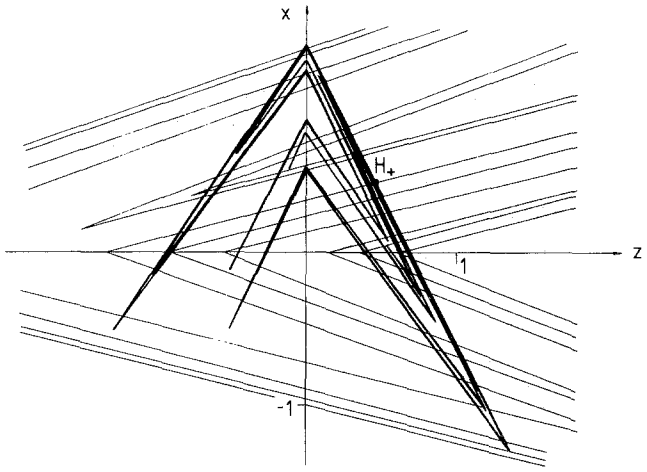

a

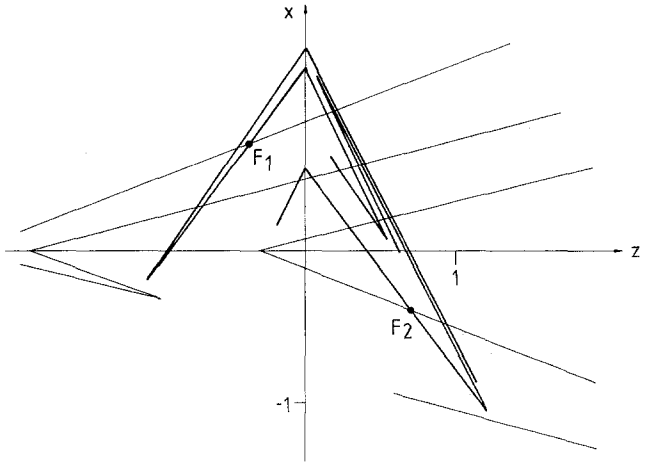

b

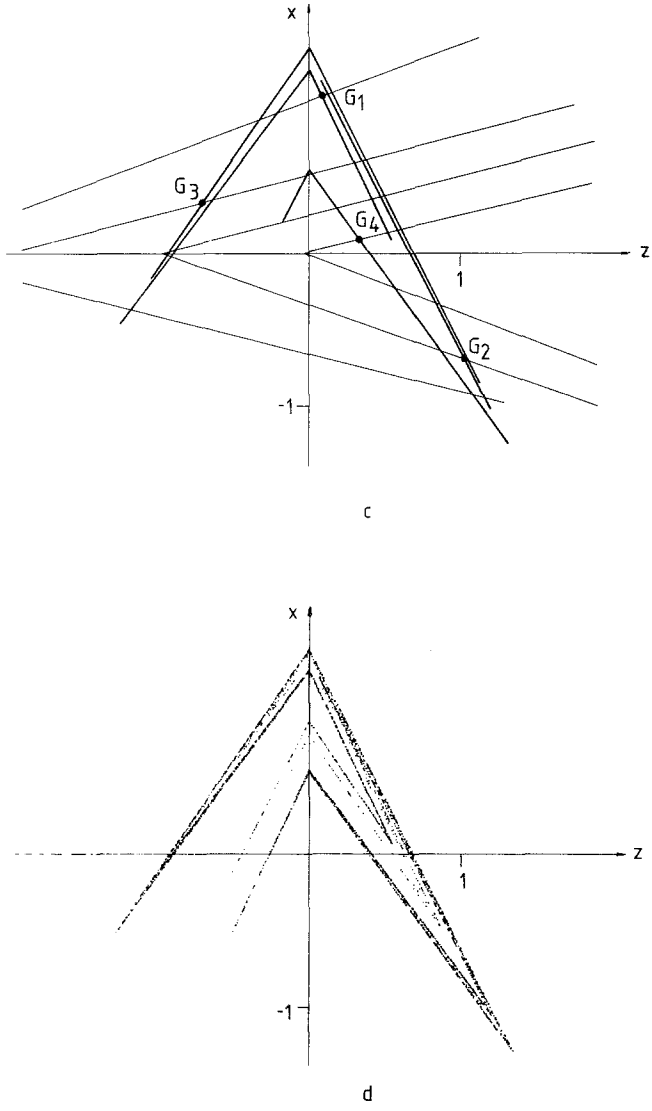

Fig. 2. At the standard values $a = 1.7$, $b = 0.5$. (a) Invariant manifolds of H_+ as obtained after five steps of construction; (b) invariant manifolds of F_1, F_2 as obtained after two steps; (c) invariant manifolds of the period-4 points $G_1, \ldots, G_4$ as obtained after one step; (d) the strange attractor in a numerical simulation after 3000 points.

Turning now to the period-2 points, one finds from (2.6) that the slopes $\lambda_{1,2}^{(2)}$ of (4.1) have to take one of the values

$$\lambda_{1,2}^{u} = \pm\left[a + (a^2 - 4b)^{1/2}\right]/2 \tag{4.7a}$$

$$\lambda_{1,2}^{s} = \pm\left[a - (a^2 - 4b)^{1/2}\right]/2 \tag{4.7b}$$

where the plus sign corresponds to the periodic point $F_1 : (x_1^{(2)}, x_2^{(2)})$. In the unstable region $a > 1 + b$, $|\lambda_{1,2}^{u}| > 1$. The slopes for both u and s fulfill the relation of being $\lambda_1\lambda_2$ just the eigenvalue (3.7) of the 2-cycle. Considering again the unstable manifolds, the straight line going through F_1 is now expected to be defined for negative values of z (remember $x_2^{(2)} < 0$), while the other one for positive values. The maximum of $f_1^*(z)$,

$$c_1^{(2)} = x_1^{(2)} - \lambda_1^{u} x_2^{(2)} \tag{4.8}$$

restricts the range of validity of f_2^* into $0 \leqslant z \leqslant c_1^{(2)}$. This means that the last point of the branch is $P_{1,1} : (1 - ac_1^{(2)}, c_1^{(2)})$, the first image of the maximum point $P_{1,0} : (c_1^{(2)}, 0)$. The inverse of f_2^*, at the same time, confines f_1^* into the region $1 - ac_1^{(2)} \leqslant z \leqslant 0$, i.e., between the points $P_{1,2}$ and $P_{1,0}$ (Fig. 1b). As long as $P_{1,2}$ lies below the z axis, the starting point of the branch going through F_2 is $P_{2,0} : (c_2^{(2)}, 0)$, its intersection point with the x axis. Similarly as in the case of the fixed points, the inverse functions are defined in a longer interval as the original functions themselves; thus (2.6) generates further branches (Fig. 1b). The stable manifolds are again to be constructed by means of (2.7).

Among the invariant curves of other periodic points we shall investigate those of the 4-cycle given by (3.10). Substituting (4.1) into (2.6) we obtain the following expressions for the slopes:

$$\begin{aligned} \lambda_1^{(4)} &= -\frac{a}{2}(1 + A), & \lambda_2^{(4)} &= -\frac{a^2 + 2b}{2a}\left(1 + \frac{1}{A}\right) \\ \lambda_3^{(4)} &= \frac{a}{2}\left(1 + \frac{1}{A}\right), & \lambda_4^{(4)} &= -\frac{a^2 - 2b}{2a}(1 + A) \end{aligned} \tag{4.9}$$

with

$$A = \left(\frac{a^2 + 2b}{a^2 - 2b}\right)^{1/2} \tag{4.10}$$

Taking $\prod_{i=1}^{4} \lambda_i^{(4)}$, it turns out to be the eigenvalue $\lambda_+^{(4)}$ specified by (3.12); thus the above choice corresponds to the unstable manifolds. The slopes of the stable ones are obtained by replacing A by $(-A)$. Further steps proceed along the same lines as in the case of period-2 points.

The construction sketched above converges: after a few steps, i.e., after a few subsequent extensions of (4.1), the new lines will lie so close to the

original one that they cannot be distinguished any more. In the case of the unstable manifolds, having a picture the size of Fig. 2, for example, one may stop after five steps of construction as further steps hardly modify the picture.

Figure 2a–c shows invariant manifolds at the standard value of parameters[8] $a = 1.7$, $b = 0.5$ where the existence of a strange attractor is proven.[11] In particular, the separatrices of the hyperbolic fixed point H_+ as well as those of the period-2 and period-4 points are presented. Each picture shows homoclinic points between the stable and unstable manifolds associated with the same hyperbolic point. It is instructive to see that the unstable separatrices of the periodic points run indeed among the branches of W_+^u, the unstable separatrix of H_+, similarly as in the Hénon model.[15] Branches of the unstable manifolds of the periodic points come, already after a few steps of construction, so close to those of W_+^u that they are scarcely to be distinquished. In fact, we had to stop after 2 (1) extensions when constructing the unstable manifolds of period-2 (4) points in order to get different pictures from Fig. 2a.

Not only these unstable separatrices are parallel to W_+^u. The unstable manifolds of each periodic points, e.g., those of the 6-cycle given by (3.13)–(3.15), are expected to run in the inside of W_+^u (the unstable manifold of H_- is winding also among the branches of W_+^u [12]). This is why the closure of W_+^u is to be considered as the strange attractor.[15] A comparison with the computer picture of Fig. 2d supports this view.

The stable manifold W_-^s of the other fixed point—not shown on Fig. 2 (see Ref. 12)—plays an important role, too. It surrounds W_+^u, as well as the separatrices of the periodic points, defining the border of the attracting region of the strange attractor.[15]

5. MODIFICATIONS OF THE STRANGE ATTRACTOR

By varying the parameters of the map, the structure of the invariant manifolds changes and, consequently, the strange attractor is changed as well. We shall fix b, the measure of the dissipation, and consider a as a control parameter.

Studies of the Hénon model suggest[15] that there are two different mechanisms leading to the destruction of a (one-piece) strange attractor. One is related to the appearance of heteroclinic points and the other one to the disappearance of homoclinic ones.

Increasing a, the end points of the unstable separatrix W_+^u come closer and closer to the stable separatrix W_-^s of the fixed point H_-. At a critical value a_c tangent points appear (if there is one, necessarily an infinite number of them should exist) and above this point the branches of W_+^u

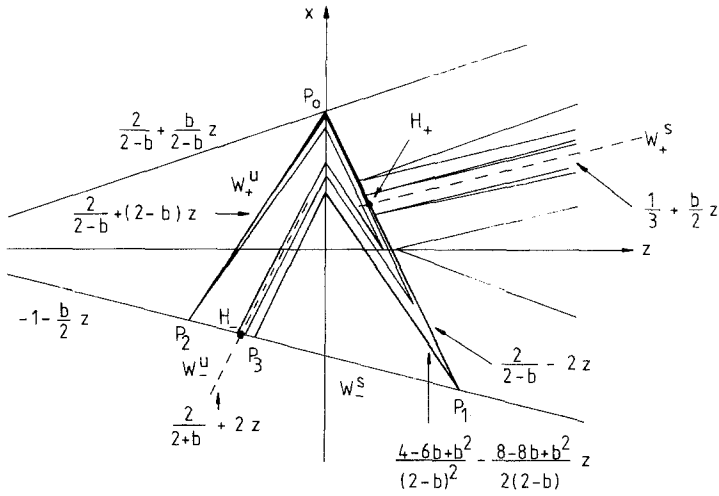

Fig. 3. Critical situation characterized by heteroclinic tangents between W_+^u and W_-^s at $a_c = 2 - b/2$.

cross W_-^s. Trajectories after crossing the curve of W_-^s go to infinity, i.e., the unstable manifold (more precisely its closure) is no more a finite attractor. In the immediate vicinity of a_c, of course, typical sequences spend quite a long time inside W_-^s before escaping.

The value of a_c can be most easily specified by considering the maximum point P_0 of W_+^u and requiring it lies on the branch (4.6) of W_-^s (Fig. 3). This gives

$$-d_-^* = c_+^* (1/\lambda_-^s + 2a_c/b) \tag{5.1}$$

where c_+^* and d_-^* have been defined by (4.2) and (4.4). Using the identities

$$-d_-^* = (b + \lambda_-^s)^{-1}, \qquad c_+^* = (1 + \lambda_-^s)^{-1} \tag{5.2}$$

one obtains

$$a_c = 2 - b/2 \tag{5.3}$$

(see also Refs. 11 and 12) involving

$$\lambda_\pm^u = \mp 2, \qquad \lambda_\pm^s = \pm b/2 \tag{5.4}$$

The images of the point P_0, i.e., $P_1, P_2, \ldots$ turn out to touch the branch (4.5) of W_-^s (Fig. 3). On the other hand, the preimages of P_0, i.e., the points $T^{-n}(P_0)$, where T^{-n} denotes the nth iterate of the inverted map, are also heteroclinic tangents. Above a_c the points P_i for $i \to \infty$ go to infinity along W_-^u, i.e., the unstable manifold of H_+ does not remain bounded.

By lowering a, the points $P_3, P_4, \ldots$ go into the inside of the triangle $P_0P_1P_2$ and at another critical value a_{c1} a situation is reached where all P_i touch the stable manifold W^s_+ of H_+. When calculating a_{c1} we use the fact that $P_1 : (1 - ac^*_+, c^*_+)$ in this case lies on the branch (4.6) of W^s_+, i.e.,

$$c^*_+ - d^*_+ = (1 - ac^*_+)(1/\lambda^s_+ - 2a_{c1}/b) \tag{5.5}$$

After substituting (4.2), (4.4), (3.3), it follows that

$$a_{c1} = \frac{1}{2}\left\{4 + 3b^2 + \left[(4 + 3b^2)^2 - 32b^3\right]^{1/2}\right\}^{1/2} \tag{5.6}$$

this result has already been obtained in Ref. 11. Let us consider now a_{c1} as a function of b. In the one-dimensional ($b = 0$) case $a_{c1} = \sqrt{2}$; the curve $a_{c1}(b)$ is slowly increasing and crosses the stability border of the 2-cycle $a^{(2)} = 1 + b$ at $b = 0.506\ldots$.

Figure 4 shows the configuration of W^u_+ and W^s_+ at a_{c1} ($b = 0.3$). The points $P_2, P_3, \ldots$ all touch the branch (4.5) of W^s_+, while P_0 belongs to another branch. The preimages of P_0 are also homoclinic tangents. When comparing Fig. 4 to the corresponding picture of the Hénon model[23] a striking topological similarity is found.

Below the critical value homoclinic points cease to exist and the feedback mechanism produced by them disappears; thus W^u_+ cannot be related any more to a strange attractor. In all cases known until now a_{c1} is the same point where heteroclinic intersections among W^s_+ and the unstable manifolds of the period-2 points disappear, thus the closure of the latter

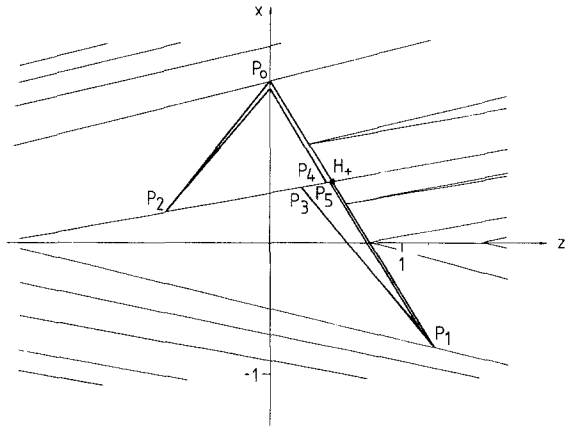

Fig. 4. Critical situation characterized by homoclinic tangents between W^u_+ and W^s_+ ($a_{c1} \cong 1.452$, $b = 0.3$, after five steps).

object may become a (two-piece) strange attractor. We shall show, however, that in decreasing the control parameter at greater values of b, the two events do not necessarily occur at the same time: heteroclinic intersections may cease earlier, resulting in the appearance of a two-piece strange attractor already above a_{c1} (see Section 6). If the splitting happens at a_{c1}, just below this value the strange attractor looks as if short pieces of W_+^u would be cut out from the neighborhood of H_+.[13]

By a further decrease of the control parameter, a subsequent critical value a_{c2} may be reached characterizing a situation with homoclinic tangents now between the separatrices of the period-2 points. Considering one part of the attractor, the configuration of the invariant manifolds is similar to that found at a_{c1}, analogously as in the case of the Hénon model.[23] Since in the region of relatively small values of the control parameter the maximum point $P_{1,0}:(c_1^{(2)},0)$ of the first branch of the unstable manifold emanating from F_1 (Fig. 1) has a second image, $P_{1,2}$, lying in the second quadrant, the end point of the second branch of the same separatrix is the fourth image, $P_{1,4}$.[13] At a_{c2} this point should touch the closest branch of the stable separatrix of F_1; thus we obtain

$$T_x^4\big(c_1^{(2)},0\big) = x_1^{(2)} + \lambda_1^s\big(T_z^4\big(c_1^{(2)},0\big) - x_2^{(2)}\big) \tag{5.7}$$

where T^4 denotes the fourth iterate of the map and other symbols have been defined in Section 4. Calculating a_{c2} at different values of b, it turns out that in the one-dimensional limit $a_{c2} = \sqrt[4]{2}$, while for b close to 1 a_{c2} approaches the stability border of the 2-cycle, the deviation being proportional to $(1-b)^2$. In the intermediate region a numerical solution shows that the curve $a_{c2}(b)$ tends to the line $a^{(2)} = 1 + b$ quite rapidly and crosses the critical curve a_{c1} at $b = 0.458\ldots$ (this is why at $a_{c1}(b = 0.5) = 1.504\ldots$ a 4-piece strange attractor can be observed), and that of a_c at $b = 0.659\ldots$ (Fig. 8).

Below a_{c2} the unstable manifolds of the period-4 points have no heteroclinic intersections with the stable manifolds of the period-2 points; thus the former objects are the most plausible candidates for representing a (4-piece) strange attractor. Figure 5 shows the unstable manifolds of the period-4 points constructed below a_{c2}, which agree well with the strange attractor obtained in a numerical simulation at the same value of the control parameter.

We have determined the next critical value a_{c3}, too, corresponding to the appearance of homoclinic tangents between the separatrices of the period-4 points. Magnifying, for example, the uppermost part, a similar situation is found as on Fig. 4. The first branch of the unstable manifold of G_1 is characterized by the slope $\lambda_1^{(4)}$ given in (4.9). The end point of the next branch is the eighth image of the maximum point $(c_1^{(4)},0)$ where

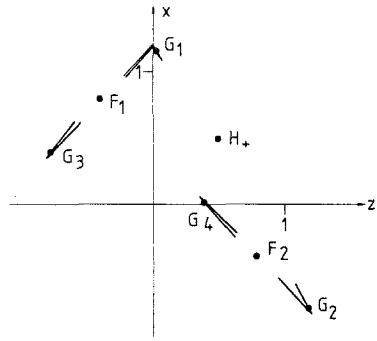

Fig. 5. Unstable manifolds of the period-4 points $G_1, \ldots, G_4$ as obtained after five steps of construction at parameter values $a = 1.52$, $b = 0.5$ ($a_{c2} \approx 1.528$).

$c_1^{(4)} = x_1^{(4)} - \lambda_1^{(4)} x_4^{(4)}$ and the coordinates of the 4-cycle have been given by (3.10). At a_{c3} the end point lies just on the stable manifold of G_1, i.e., the equation

$$T_x^8\left(c_1^{(4)}, 0\right) = x_1^{(4)} - a_{c3}(1 - A)\left(T_z^8\left(c_1^{(4)}, 0\right) - x_4^{(4)}\right)/2 \qquad (5.8)$$

is to be fulfilled, where A is defined by (4.10). The curve $a_{c3}(b)$ starts at $\sqrt[8]{2}$. According to the numerical solution it increases slowly and, in contrast to $a_{c2}(b)$, crosses the line $a^{(2)} = 1 + b$ (Fig. 8). The point of intersection is at $b = 0.133\ldots$. Just below a_{c3} an eight-piece strange attractor is expected.

In the one-dimensional limit the strange attractor goes through an infinite sequence of doubling bifurcations. It is easy to show that the splitting from 2^{k-1} to 2^k chaotic bands occurs at $a_{ck} = 2^{2^{-k}}$. The results above suggest, however, a breakdown in the sequence of doubling bifurcations after a finite number of steps when decreasing a at finite values of b.

6. STRUCTURAL INSTABILITY OF THE UNSTABLE MANIFOLDS OF THE PERIOD-2 POINTS; THE PHASE DIAGRAM OF THE MAP

The picture emerging from the previous sections is not yet complete. The fact the curve of a_{c2} crosses that of a_{c1} poses the question of what type of attractor appears just above a_{c2} for relatively great values of b. Numerical simulations show that in a small band above a_{c2} a two-piece strange attractor exists in the whole region of interest. By increasing a at a fixed b this strange attractor abruptly turns into a one-piece one, as long as $a < 2 - b/2$, otherwise a region without finite attractors is reached.

In order to explain the phenomenon, let us consider the invariant manifold of the fixed point H_+ and those of the period-2 points at the critical value a_{c1} for $b = 0.4$. The result of the construction is shown on Fig. 6a. Homoclinic tangents characterize the configuration of the separatrices of H_+, but, quite surprisingly, the unstable manifolds of the period-2 points do not follow entirely the branches of W^u_+ and have no heteroclinic

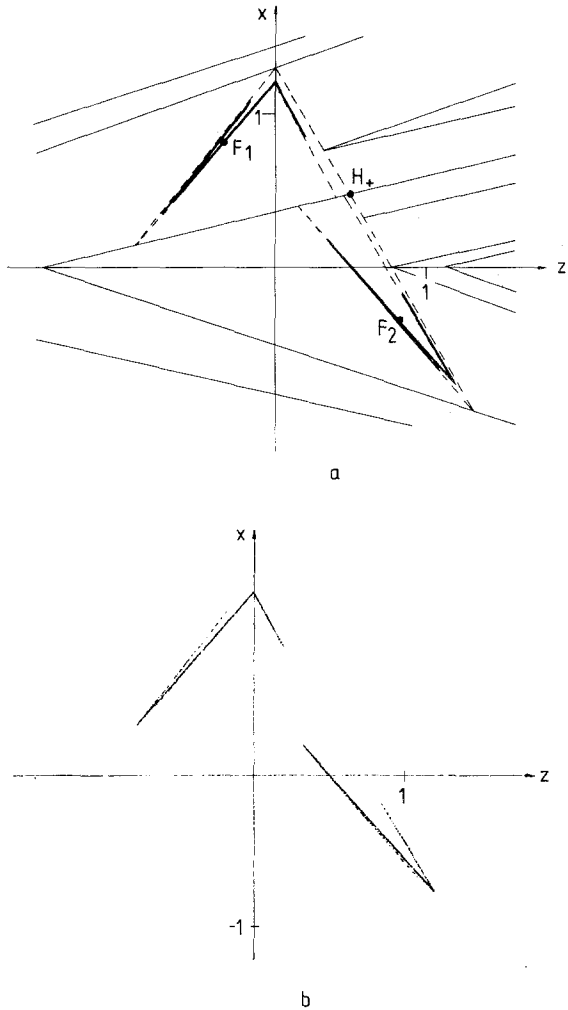

Fig. 6. (a) Separatrices W^u_+ (dashed), W^s_+ (solid) emanated from H_+, and the unstable manifolds of the period-2 points (thick) at $a_{c1} \cong 1.476$, $b = 0.4$ (after five steps); (b) the strange attractor at the same values obtained in a numerical simulation after 3000 points.

intersections with W_+^s. On the other hand, the unstable separatrices of period-4 points run indeed between the branches of those of period-2 points. Assuming that this happens with the unstable manifolds of other periodic points, too, we conclude that in this case the closure of the unstable manifolds of the period-2 points gives already the strange attractor. This is supported by the numerical results (Fig. 6b). The heteroclinic intersections with the stable manifolds of the period-2 points destroy the attracting character of W_+^u.

The typical features of this example are the following. At certain values of the parameters it may happen that the branches of the stable manifold W_+^s do not come close to the period-2 points. On the other hand, the unstable manifolds of the period-2 points have two structurally different forms: a less compact one, which is qualitatively similar to that of W_+^u, and a more compact one which only partially follows the branches of W_+^u. If the more compact form fits into the region left intact by W_+^s, i.e., no heteroclinic points are present, the closed set of the unstable manifolds of the period-2 points can be a strange attractor in spite of the fact that homoclinic points between W_+^s and W_+^u still exist.

To find a condition for the structural instability of the unstable manifolds of period-2 points occurring at some value a'_{c1}, let us consider the cases of $a = 1.55$ and $a = 1.56$ at $b = 0.5$ (Fig. 7a, b). While in the first case the shape of the manifolds does not change considerably after the first six steps, branches become effectively elongated by further and further steps in the second case and the final form will have several intersection points with the stable manifold W_+^s. At an intermediate value of a we arrive at a situation where $P_{1,3}$ and $P_{1,9}$, $P_{1,4}$, and $P_{1,10}$, ... are close to each other. More precisely, the end points of the branches come close to the points of a 6-cycle; they are suspected to touch the stable manifolds of this 6-cycle in the critical case. The situation is quite similar to the structural instability of W_+^u at a_c.

In specifying a'_{c1} there is a difficulty since $P_{1,0}: (c_1^{(2)}, 0)$ is not the exact maximum point of the unstable manifold; in fact the branch ending at $P_{1,9}$ generates a point above $P_{1,0}$, etc. For values of b, not immediately close to 1, however, the difference is small and we obtain an approximate value for a'_{c1} by requiring $P_{1,4}$ to be in the same height as the 6-cycle point given by (3.13), (3.15), i.e.,

$$T_x^4\left(c_1^{(2)}, 0\right) = x_1^{(6)} \tag{6.1}$$

The curve $a'_{c1}(b)$ obtained in this way starts from $((1+\sqrt{5})/2)^{1/2} = 1.272\ldots$ at $b = 0$ and crosses the line $a_{c1}(b)$ at $b = 0.382\ldots$. For $b = 0.5$ Eq. (6.1) gives $a'_{c1} = 1.556\ldots$, while the result of the computer simulation is $a'_{c1} = 1.555\ldots$. For greater values of b the accuracy is decreasing

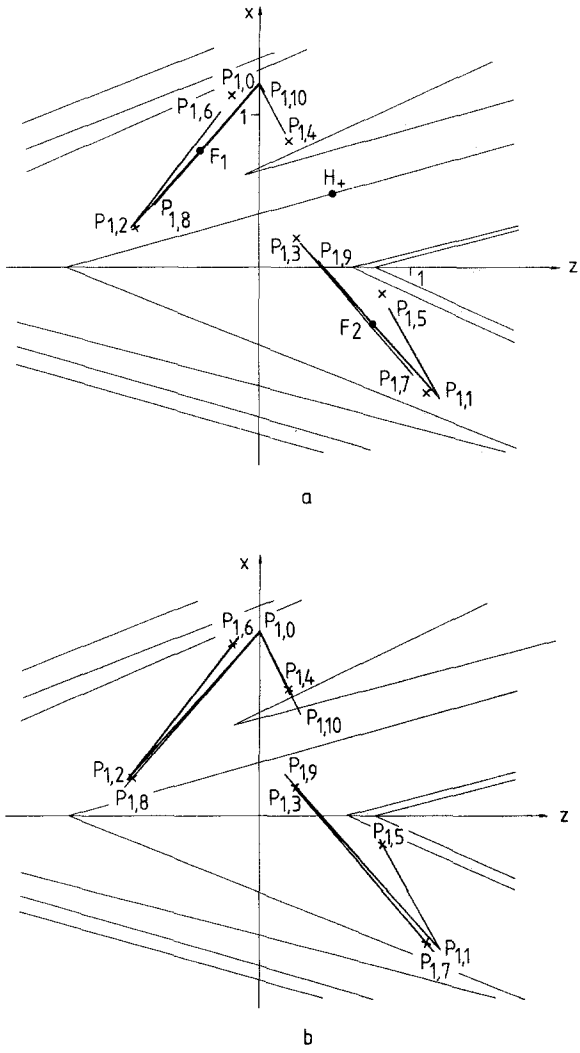

Fig. 7. Unstable manifolds of the period-2 points as obtained after six steps of construction. $b = 0.5$ (a) $a = 1.55$, (b) $a = 1.56$. Crosses denote period-6 points. A few branches of W^s_+ are shown, too.

but the approximate curve (Fig. 8) properly expresses the tendency that a'_{c1} approaches a_{c2} as b goes to 1.

Now we can locate the region of the most important attractors on the phase diagram. As the numerical simulations show typically only one attractor for a given parameter value, we can summarize the results as

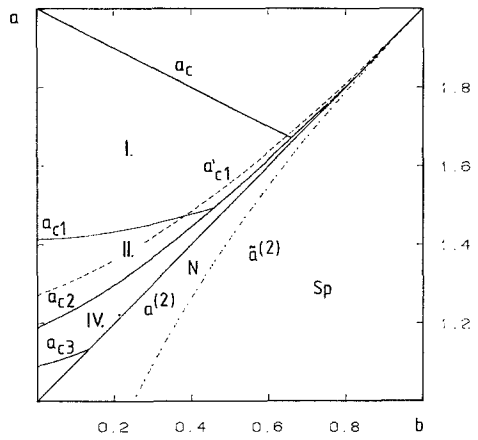

Fig. 8. Phase diagram of the piecewise linear map. Regions I, II, and IV belong to 1-, 2- and 4-piece strange attractors, respectively. The dashed–dotted line ($\tilde{a}^{(2)} = 2\sqrt{b}$) separates regions N and Sp where the 2-cycle points are stable nodes and spirals, respectively.

follows. Below $a_c = 2 - b/2$ and above the maximum of a_{c1} and a'_{c1} a one-piece strange attractor exists (Fig. 8). Below the maximum of a_{c1} and a'_{c1} a two-piece strange attractor appears with qualitatively different shapes near a_{c1} and a'_{c1}. The lower borderline of this region is a_{c2}. We cannot exclude the possibility that a similar structural instability, as discussed above, occurs in the unstable manifolds of other periodic points, too, but according to our numerical investigations the deviation from the critical lines calculated in Section 5 must be small. Thus, the region for the 4-piece strange attractor is expected to lie below a_{c2} and above the maximum of the curves a_{c3} and $a^{(2)}$. Below the straight line $a^{(2)} = 1 + b$ no strange attractor exists. The 2-cycle points are stable nodes in region N and stable spirals in region Sp (Fig. 8).

Finally, we note that in contrast to the case of the Hénon model we have not found an alternation of periodic and strange attractors when varying the control parameter. This can be traced back to the fact that in the one-dimensional map $x_{n+1} = 1 - a|x_n|$ periodic windows do not appear, the Lyapunov number, $\ln a$, is positive for all $a > 1$.

7. THE CONSERVATIVE CASE

A typical computer picture obtained in the limit $b = 1$ is shown on Fig. 9. The dots belong to chaotic sequences of unbounded trajectories, while the closed curves are associated with the 2-cycle (points jump between two tori of the same size). This can be understood by observing on

the one hand that as $b \to 1$ both manifolds of the fixed points become unbounded and leave out two holes around the period-2 points, and on the other hand that the 2-cycle points become elliptic for $b = 1$ as follows from (3.7).

The method of construction of stable and unstable manifolds remains valid in the conservative limit, too, although the convergence of the construction is slower than in the dissipative case. Figure 10a shows W_+^u obtained after ten steps of construction at the same value of the control parameter as on Fig. 9, while Fig. 10b shows the corresponding stable manifold W_+^s obtained after six steps. When the two pictures are laid on top of one another, a great number of homoclinic points emerge. Topologically similar pictures have been found in the conservative Hénon model,[27–29] too. Note, that the manifold W_-^s can be obtained from W_+^u by the simple transformation (2.9), and W_-^u similarly from W_+^s.

The form of the invariant curves of the period-2 points follows also from Eq. (2.6). The curves should belong to a family with the property that adding $f(z)$ to the inverse of a curve around $F_1 : (1/a, -1/a)$ one obtains the curve around $F_2 : (-1/a, 1/a)$, and vice versa. As long as only one of the straight lines of $f(z)$ is needed in this procedure, the closed curves can

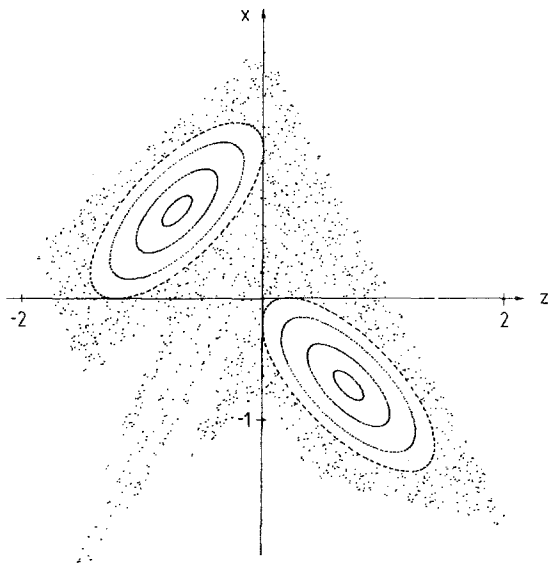

Fig. 9. Computer picture of the piecewise linear map in the conservative limit. Dots belong to unbounded chaotic trajectories. The tori are invariant curves of the period-2 points ($a = 1.4$, $b = 1$).

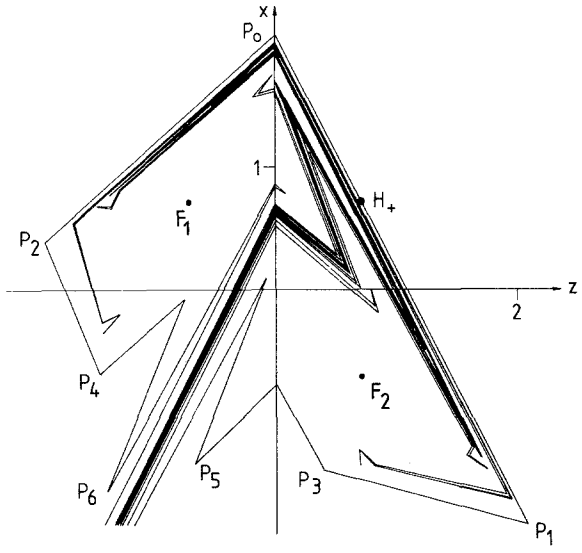

a

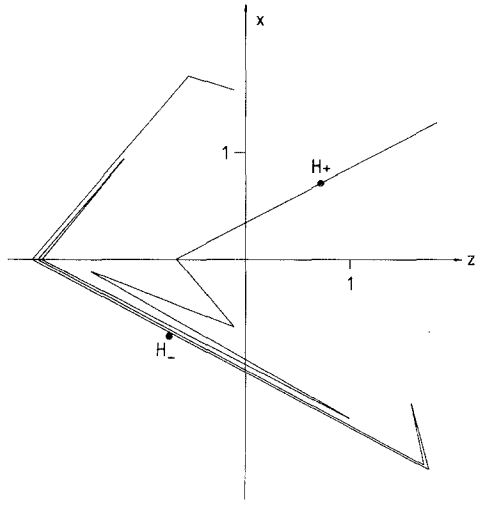

b

Fig. 10. (a) The unstable separatrix W_+^u as obtained after ten steps of construction; (b) the stable separatrix W_+^s as obtained after six steps of construction ($a = 1.4$, $b = 1$).

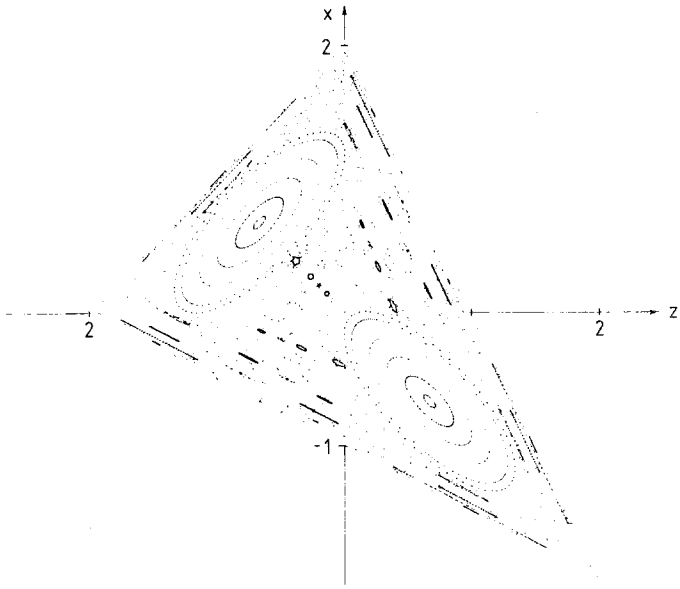

Fig. 11. Computer picture of the critical situation at $a_c = 1.5$. The small tori are invariant curves of period-8, -10, -12, -14 points.

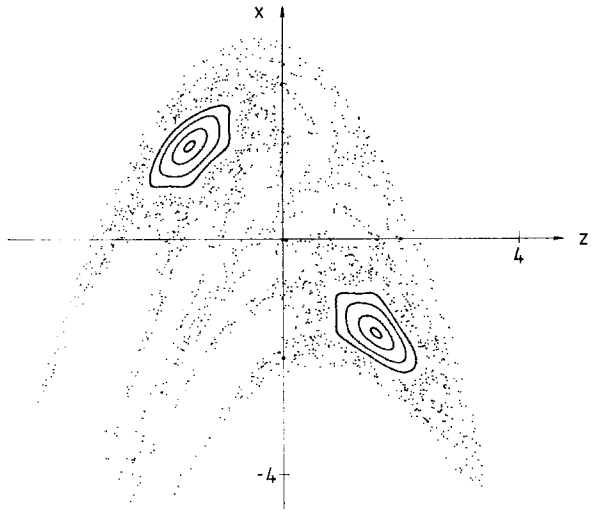

Fig. 12. Computer picture of the Hénon model in the conservative limit $b = 1$. Dots belong to unbounded trajectories. The tori are invariant curves of the period-2 points ($a = 0.4$).

be ellipses. They fulfill the symmetry relation (2.10) only if the main axes are parallel to the diagonals. Thus their equation reads

$$\left(x \mp \frac{1}{a}\right)^2 \mp 2\frac{\kappa - 1}{\kappa + 1}\left(x \mp \frac{1}{a}\right)\left(z \pm \frac{1}{a}\right) + \left(z \pm \frac{1}{a}\right)^2 = \frac{2a'^2}{\kappa + 1} \tag{7.1}$$

with

$$\kappa = a'^2/b'^2 \tag{7.2}$$

where a' and b' denote the two semiaxes of the ellipses. The upper sign in (7.1) belongs to a curve located around F_1, and the lower sign to that around F_2. The condition expressed by (2.6) specifies the value of κ as

$$\kappa = \frac{2 + a}{2 - a} \tag{7.3}$$

The outermost ellipse touching the x and z axes is characterized by

$$a'_{\max} = \left(\frac{2 + a}{2a^2}\right)^{1/2} \tag{7.4}$$

Consequently, within the region bounded by the outermost ellipse the motion is regular, the invariant tori are concentric ellipses given by the form of (7.1) and (7.3). The numerical simulations suggest that the region of chaotic sequences comes close to the outermost ellipse. [In the limit $a \to 2$ the ellipses are deformed into two pieces of straight lines joining the points $(0, -1), (1, 0)$, and $(0, 0), (-1, 1)$.]

Finally, two remarks are in order.

As Fig. 10a shows, at $a = 1.4$ the points P_3, P_4 lie below the line $\overline{P_2P_1}$. Increasing the control parameter, however, the positions can change. There is a critical configuration at $a_c = 1.5$ [note that this is just the limiting value of (5.3)] where $P_3, P_4 \ldots$ touch the line $\overline{P_2P_1}$. Then, W^u_+ and W^s_- coincide and form a triangle with corner points $(2, 0), (0, -2), (-2, 2)$. It is now a closed invariant curve of the map. Thus, chaotic trajectories starting from the inside of the triangle are confined into this region (Fig. 11), which gives a special importance to this case.

Based on the similarities between the topological structure of the invariant curves of the piecewise linear map and that of the Hénon model, one may ask whether it is possible to find the analogous picture of Fig. 9 in the conservative limit of the Hénon model, $b = 1$ in (2.1), (2.4) (note that the canonical form of Hénon's conservative map corresponds to the choice $b = -1$ in our representation[1]). The answer is affirmative. Figure 12 is the result of the computer simulation at $a = 0.4$. The invariant curves should have the property that adding a parabola to the inverse of one of them gives just the other one. The borderline of the dotted region of chaotic

sequences is expected to be given by the first branches of the unstable manifold of the fixed point H_+ lying in the first quadrant. The configuration is similar to that found for $a > a_c = 1.5$ in the piecewise linear map.

ACKNOWLEDGMENT

The author is indebted to Prof. R. Graham for illuminating discussions and kind hospitality, to Prof. P. Szépfalusy for several helpful comments, and to Prof. D. Ter Haar for drawing his attention to Ref. 27. Dr. M. Dörfle's help in introducing the author to the use of the computer is highly acknowledged. Thanks are due to Drs. J. Haus and G. Györgyi for a critical reading of the manuscript.

REFERENCES

1. R. H. G. Helleman, in *Fundamental Problems in Statistical Mechanics*, E. G. Cohen, ed. (North-Holland, Amsterdam, 1980), Vol. 5, pp. 165–233.
2. K. Tomita, *Phys. Rep.* **86**:113 (1982).
3. J. L. Kaplan and J. A. Yorke, *Lecture Notes in Math.* **730**:228 (1979).
4. R. V. Jensen and C. R. Oberman, *Phys. Rev. Lett.* **46**:1547 (1981).
5. D. Mayer and G. Roepstorff, Strange atrractors and asymptotic measures of discrete-time dissipative systems, preprint (Aachen, 1982).
6. E. Ott and J. D. Hanson, *Phys. Lett.* **85A**:20 (1981).
7. R. Graham, Exact solution of some discrete stochastic models with chaos, preprint (Essen, 1982).
8. R. Lozi, *J. Phys. (Paris)* **39**:C5, 9 (1978); in *Intrinsic Stochasticity in Plasmas*, G. Laval and D. Gresillon, eds. (Edition de Physique, Orsay, 1979), pp. 373–381.
9. M. Hénon and Y. Pomeau, *Lecture Notes in Math.* **565**:29 (1976).
10. M. Hénon. *Commun. Math. Phys.* **50**:69 (1976).
11. M. Misiurewicz, in *Nonlinear Dynamics, Annals of the New York Academy of Sciences*, Vol. 357, R. H. G. Helleman, ed. (New York Academy of Sciences, New York, 1980) pp. 348–358.
12. T. Tél, *Z. Phys.* **B49**:157 (1982).
13. T. Tél, *Phys. Lett.* **94A**:334 (1983).
14. R. Lozi, in *Théorie de l'iteration et ses applications*, R. Thibault, ed. (Edition du CNRS, Toulouse, 1982), pp. 145–152.
15. C. Simó, *J. Stat. Phys.* **21**:465 (1979).
16. P. Holmes, *Philos. Trans. R. Soc.* **A292**:419 (1979).
17. Y. Ueda, *J. Stat. Phys.* **20**:181 (1979).
18. H. Daido, *Prog. Theor. Phys.* **63**:1190 (1980).
19. S. D. Feit, *Commun. Math. Phys.* **61**:249 (1978).
20. J. H. Curry, *Commun. Math. Phys.* **68**:129 (1979).
21. F. R. Marotto, *Commun. Math. Phys.* **68**:187 (1979).
22. C. Tresser, P. Coullet, and A. Arneodo, *J. Phys.* **13A**:L123 (1980).
23. P. Collet and J. P. Eckmann, *Iterated Maps on the Interval as Dynamical Systems* (Birkhäuser, Basel, Boston, 1980).
24. V. Francheschini and L. Russo, *J. Stat. Phys.* **25**:757 (1981).

25. P. Manneville, *Phys. Lett.* **90A**:327 (1982).
26. P. Bridges and G. Rowlands, *Phys. Lett.* **63A**:189 (1977).
27. E. M. McMillan, in *Topics in Modern Physics*, W. E. Brittin and H. Odabasi, eds. (Adam Hilger, London, 1971), pp. 219–244.
28. M. V. Berry, in *Topics in Nonlinear Dynamics*, American Institute of Physics Conference Proceedings, Vol. 46, S. Jorna, ed. (American Institute of Physics, New York, 1978), pp. 16–120.
29. L. J. Laslett, in *Topics in Nonlinear Dynamics*, American Institute of Physics Conference Proceedings, Vol. 46, S. Jorna, ed. (American Institute of Physics, New York, 1978), pp. 219–244.